

The Ozone Mapping and Profiler Suite (OMPS): On-Orbit Calibration Design

Q.P. Remund^{*a}, D. Newell^a, J.V. Rodriguez^a, S. Asbury^a, G. Jaross^b

^aBall Aerospace & Technologies Corp.; ^bScience Systems and Applications, Inc.

ABSTRACT

The Ozone Mapping and Profiler Suite (OMPS) will collect total column and vertical profile ozone data and continue the daily global data produced by the current operational satellite monitoring systems, the Solar Backscatter Ultraviolet radiometer (SBUV/2) and the Total Ozone Mapping Spectrometer (TOMS), but with higher fidelity. The collection of this data will contribute to fulfilling US treaty obligations to monitor ozone depletion for the Montreal Protocol. OMPS has been selected to fly on the National Polar-Orbiting Operational Satellite System (NPOESS) spacecraft – the next generation of polar orbiting environmental satellites. The first OMPS flight unit will fly on the NPOESS Preparatory Project (NPP) spacecraft. On-orbit calibration of the OMPS instruments is critical to maintaining quality data products. A number of signal corrections and calibrations are applied on-board the sensor and in ground processing to account for instrument non-idealities and to convert measured digital signals to calibrated radiances and irradiances. Three fundamental on-orbit calibration measurements are made to provide the required data to perform the radiometric calibration and trending.

1. INTRODUCTION

A key requirement of the National Polar-orbiting Operational Environmental Satellite System (NPOESS) is the operational retrieval of total column and profile ozone products^{1,2}. The Ozone Mapping and Profiler Suite (OMPS) is designed to meet that requirement. OMPS consists of a nadir sensor and a limb profile sensor. The nadir sensor is comprised of a telescope and two spectrometers³. The spectrometers use dispersive gratings to provide the wavelength coverage required for the nadir total column (300-380 nm) and the nadir profile instrument (250-310 nm). Total column observations are collected over the full 110 degree field-of-view of the nadir sensor while nadir profile observations are taken only for the central 16 degrees. The nadir sensor will continue the heritage ozone observations made by TOMS⁴ and SBUV⁵. On the other hand, the limb sensor consists of a telescope and a spectrometer which utilizes a prism as the dispersive element to achieve wavelength coverage from 290-1000 nm⁶. The limb sensor observes radiances from the tropopause up to 60 km for the retrieval of high vertical resolution ozone profiles. The fundamental limb scattering technique was demonstrated by the Shuttle Ozone Limb Sounding Experiment / Limb Ozone Retrieval Experiment (SOLSE/LORE) flown on STS-87 in December 1997^{7,8}. CCD detectors are used in all three focal plane designs.

The OMPS sensor data are transmitted to ground processing stations for the implementation of calibration, geolocation, and ozone retrieval algorithms. The sensor data record (SDR) algorithm performs the required calibration and geolocation operations. This is followed by environmental data record (EDR) processing to estimate the total column and profile ozone products.

2. ON-ORBIT CALIBRATION OF OMPS

On-orbit calibration of the OMPS sensors ensures long-term data quality and EDR performance compliance. The fundamental calibration approach for the OMPS instruments is based upon heritage TOMS and SBUV/2 approaches^{9,10,11}. The primary objectives of the OMPS calibration are three-fold:

- Provide and apply the calibration data required to meet top-level EDR performance
- 2. Trending
- 3. Monitoring

The first, and foremost objective is providing high-quality calibration information for use in the on-orbit data corrections and the ground-based SDR algorithm. The SDR algorithm applies the pre-launch measured calibration coefficients as well as the on-orbit measurements to ensure that the calibrated albedos passed to the EDR algorithm are of sufficient quality to retrieve the required atmospheric ozone products. This topic is covered in much more depth in sections that follow.

The second objective is comprised of long-term trending of sensor characteristics. The weekly on-orbit calibration data is stored in trending databases on the ground to adjust key calibration parameters that change over time due to long-term sensor degradation. These parameters include overall radiometric albedo, pixel-to-pixel albedo, and spectral registration. Radiometric albedo is trended to watch for long-term changes in the radiance/irradiance ratios that are used in the EDR retrieval algorithms. In addition, multiple pixels are binned (co-added) together on-orbit to meet the data rate requirements during earth radiance observations. The flight software performs pixel-to-pixel gain corrections before this binning occurs. Consequently, accurate knowledge and trending of the pixel-to-pixel variability is important. Trending of the spectral registration on the focal plane is also performed in order to track and correct for long-term variations in the spectral calibration of each of the instruments. For each of these three trended parameters, the ground processing algorithms use the most recent 10-15 weeks of data to extrapolate the appropriate values for the next week. The extrapolated values are used during the operational processing and calibration until the next weekly calibration occurs at which time the process begins again. Of course, retrospective processing will allow for more accurate, but less timely calibration with data that are interpolated in the trending rather than extrapolated.

The final objective of the on-orbit calibration of the OMPS system is monitoring. The monitoring process is intended to maintain watches on parameters that are not expected to vary on weekly timescales. Rather, the monitoring is used to track various performance parameters for quality assurance and to make periodic adjustments in the processing to compensate for any observed changes. Key parameters that are monitored are diffuser degradation, linearity, and bad pixels. Diffuser degradation is tracked through the use of a two-diffuser system. The weekly calibrations employ a “working” diffuser. A second “reference” diffuser is deployed only once every six months. Due to the regular exposure to UV radiation and the resulting photo-polymerization of contaminants, the working diffuser tends to degrade much more quickly than the reference diffuser which is protected from UV radiation except for the semi-annual deployments. The diffuser monitoring approach has been shown to work for previous sensors such as TOMS, SBUV, and SBUV/2^{12,13}. The nonlinearity is monitored through weekly LED measurements to track any long-term degradation in the performance of the CCD and electronics amplifiers. Finally, various on-orbit calibration measurements are used to detect bad pixels including excessive dark current and low pixel responsivity. Both of these phenomena can result from long-term radiation damage to the CCD. If a pixel is determined to be above the defined bad pixel limits, it is subsequently removed from the on-orbit binning to minimize impacts on top-level EDR performance.

The stated objectives are met through the measurement and application of on-orbit calibration data including solar observations, dark current measurements, and LED illumination of the CCD. The sections below define the on-orbit calibration driving requirements, the specific corrections and calibrations, and the on-orbit calibration systems and processes.

2.1. Driving requirements

Table 1 contains the OMPS on-orbit calibration requirements for both the nadir and limb profile sensors. The table defines the term, the associated required value, and the key processes or suballocations which are driven by a each requirement. Wavelength independent albedo calibration captures correlated errors over all wavelengths in the OMPS sensor spectra. This term primarily drives the trending and goniometry processes. On the other hand, the wavelength dependent calibration term accounts for calibration effects that vary across the spectra in an uncorrelated manner. The wavelength dependent term drives trending as well as the solar irradiance signal-to-noise ratio (SNR). The wavelength monitoring accuracy term constrains the allowed on-orbit spectral registration knowledge. Since the solar measurements are used for this term, this term also drives solar SNR. The last requirement, pixel-to-pixel radiometric calibration accuracy is comprised of residual errors following the signal corrections which are computed before the radiometric calibration coefficients are applied. The pixel corrections draw on data from all three of the fundamental calibration measurements. As a result, they drive properties of the solar irradiance, dark current, and LED observations.

These key requirements drive the design and methodologies that are necessary to ensure proper on-orbit calibration of the OMPS sensors.

Table 1. On-orbit calibration driving requirements.

| Parameter | Required Value | Drives |
|---|--------------------------------------|-------------------------|
| Nadir | | |
| Long-term albedo calibration (wavelength independent) | <0.5% | Trending and goniometry |
| Long-term albedo calibration (wavelength dependent) | <0.3% | Trending and solar SNR |
| Wavelength monitoring accuracy | 0.01 nm | Solar SNR |
| Pixel-to-pixel radiometric calibration accuracy | <0.5% | Solar, Dark, LED data |
| Limb | | |
| Long-term albedo calibration (wavelength independent) | 0.5% (28-60 km) 0.25% (TP-28 km) | Trending and goniometry |
| Long-term albedo calibration (wavelength dependent) | 0.25% (28-60 km) 0.13% (TP-15 km) | Trending and solar SNR |
| Wavelength calibration accuracy | <0.03 FWHM (Vis) <0.01 FWHM (UV) | Solar SNR |
| Pixel-to-pixel radiometric calibration accuracy | <0.4% | Solar, Dark, LED data |

2.2. Signal corrections and calibration

The OMPS instruments each take separate measurements of earth radiances as well as weekly measurements of solar irradiance. The EDR algorithms then use the radiance/irradiance ratios, also called albedos, to retrieve the various ozone products. The use of albedos reduces sensitivity to long-term sensor degradation. In addition, the albedos remove the effects of solar variations that occur on timescales which are longer than a week. The SDR algorithm performs calibrations on the earth radiance and solar irradiance terms separately. The radiance calibration is given by the following equation:

$$L_{jk}^m(t) = \frac{Q_{jk}^r k_{jk}^r}{\tau_{jk}(t)}$$

Q_{jk}^r = the corrected earth radiance counts (digital number) for the pixel (j,k)

k_{jk}^r = the pre-launch measured radiance calibration coefficient for the pixel

$\tau_{jk}(t)$ = sensor response changes as a function of time t

L_{jk}^m = the resulting calibrated earth radiance.

The sensor response change term is one by definition at launch. It is then used to trend long-term throughput changes of the OMPS instruments. The signal corrections that result in Q_{jk}^r require the on-orbit solar irradiance, dark current, and LED measurements.

In a similar manner, the weekly solar irradiance measurements are calibrated. The fundamental irradiance calibration equation is:

$$E_{jk}^m(t) = \frac{Q_{jk}^i k_{jk}^i}{g_{jk}(\theta, \phi) \rho_{jk}(t) \tau_{jk}(t)}$$

Q_{jk}^i = the corrected solar irradiance counts for pixel (j,k)

k_{jk}^r = the pre-launch measured irradiance calibration coefficient

$g_{jk}(\theta, \phi)$ = the goniometric response at solar angle (θ, ϕ)

$\rho_{jk}(t)$ = the long-term solar diffuser reflectivity (nadir sensor) or transmissivity (limb sensor) changes

E_{jk}^m = the calibrated solar irradiance.

The two new terms that appear in this equation, g and ρ , are needed to characterize the solar diffuser used in solar irradiance measurements. The irradiance calibration coefficients and the goniometry are measured in pre-launch calibrations of the OMPS instruments. Like the throughput term, the diffuser reflectivity or transmissivity is one at launch. The working diffuser characteristics are then trended over time through the periodic use of the reference diffuser. The corrected counts are computed using the three fundamental on-orbit calibration measurements.

While the SDR algorithm performs separate calibrations on earth radiances and solar irradiances, the EDR algorithm uses irradiance-normalized radiances in the retrieval. In effect, the ozone retrieval algorithms operate on data that has been calibrated in the following manner:

$$\frac{L_{jk}^m}{E_{jk}^m} = K_{jk} \frac{Q_{jk}^r}{Q_{jk}^i} g_{jk} \rho_{jk}(t)$$

where K_{jk} is the albedo calibration coefficient (equivalent to the ratio of the radiance and irradiance coefficients).

The benefit of the albedo approach is evident in the absence in this equation of $\tau_{jk}(t)$ which represents the long-term sensor throughput degradation. Since this term cancels in the ratio, the albedos are much less sensitive to such sensor effects. In essence, the albedos are self-calibrating with respect to sensor throughput degradation that occurs on scales much longer than the period between solar calibrations.

As noted above, various signal corrections are required before the radiometric calibration can be performed. The corrections account for various non-idealities of the OMPS detectors and the associated electronics. A simplified correction equation is given as,

$$Q_c[j, k] = \frac{Q_{ADC}[j, k] - Q_0}{g(Q_{ADC}[j, k])m[j, k]} - Q_w[k] - Q_{dark}[j, k]$$

where

$Q_{ADC}[j, k]$ = the raw digital counts at the output of the on-board analog-to-digital converter (ADC)

Q_0 = the zero-input response of the CCD amplifier and the subsequent electronics

g = the non-linearity of the electronics chain (which is a function of raw signal level)

$m[j, k]$ = the relative pixel gain level due to photo-response non-uniformity (PRNU) and throughput changes

$Q_w[k]$ = the observed smear signal for column k

$Q_{dark}[j, k]$ = the observed dark signal.

The zero-input offset measurement are collected from serial buffer pixels that are measured in the solar calibrations or in the dark current frames. The buffer pixels, in theory, contain no charge and are a measure of the amplifier output in the absence of any signal. Alternatively, the smear measurements inherently contain the offset and can be used to correct for both offset and smear simultaneously.

The non-linearity in the system is caused by imperfect gain responses of various amplifiers in the OMPS instruments. The resulting effect is that the observed digital counts are not exactly proportional to the number of electrons collected in a given pixel. Component testing indicates that the bulk of the nonlinearity comes from the on-chip CCD amplifiers. An estimate of the nonlinearity curve is derived from the weekly LED data. The LED measurements are collected at stepped integration times in an effort to characterize the nonlinearity of the system over the full dynamic range of the system. Since multiple frames of data are co-added (in time) on-board the sensor and since the scene radiances change with time, this correction must be applied on the sensor before the co-adding occurs. More detail is provided in a later section.

Relative pixel gain level is dominated primarily by pixel photo-response non-uniformity (PRNU). In addition, slowly varying sensor throughput over wavelength and field angle also contributes. PRNU is a measure of the variability in quantum efficiency of CCDs at a given wavelength. Solar irradiance observations are used to measure the pixel-to-pixel variability. These data offer a relatively stable signal with high SNRs to measure small variations between pixels in a localized area. The data are binned on-orbit by summing multiple pixels within predefined “macropixels” in order to meet system data rate requirements. The binning occurs in the spatial dimension for the nadir instruments (to maintain fine spectral resolution) and in the spectral dimension for the limb instrument (to maintain fine spatial resolution). Since the correction of interest cannot be made after the binning occurs, it is applied in the on-board processor before the pixel binning operation. Initial variability is measured by the pre-launch calibration coefficients. The relative variability within each macropixel is then tracked on-orbit using the solar irradiance observations.

Since the OMPS instruments are shutterless, smearing occurs in the collected CCD frames. The smearing results from the photon flux incident upon the pixels during the parallel charge transfer operations. While the transfer occurs quickly to minimize smear, the smear signal is still large enough to warrant a correction. To measure the smear, 20 additional over-clocked pixel transfers are performed. This results in 20 “virtual pixels” that trail the original physical pixels. The extra pixels collect smear signal during their transit across the OMPS CCD. Consequently, every earth radiance or calibration frame inherently contains an estimate of the smear associated with the signal of interest. The central 16 smear pixels are used to compute an average smear signal for each CCD column. Two pixels are discarded at each end of the smear pixels to avoid transient effects which are typically observed in CCDs.

Another inherent characteristic of CCDs is dark current. Dark current results from thermally generated charge collected in CCD pixels as well as the serial registers. The dark current estimates are obtained from weekly dark current measurements for each of the OMPS focal planes. The mean dark signal is subtracted off for each macropixel during the SDR signal corrections. The random noise associated with dark current cannot be corrected and results in reduced SNR.

Spectral registration is another key component of the OMPS calibration process. The three spectrometers disperse light onto each of the focal planes over the required range of wavelengths. Over time, the spectral illumination can shift slightly requiring periodic re-registration. The spectral calibration is based on an approach derived by Caspar and Chance¹⁴ and relies upon well-known solar Fraunhofer absorption lines. With knowledge of the position of these lines, solar irradiance data are fit to the theoretical solar spectrum to determine the wavelength of each pixel on the focal plane. For proper spectral calibration to occur, the solar irradiance data must exhibit low noise to clearly measure the absorption lines.

2.3. On-orbit calibration measurements

Each of the corrections and calibrations noted above draw on various pre-launch measurements as well as on-orbit weekly calibration observations. Solar irradiance, dark current, and LED illumination observations all provide critical inputs to the on-orbit calibration process.

2.3.1. Solar irradiance calibration

The OMPS instruments collect solar irradiance measurements weekly. The primary use of the solar irradiance observations is in the generation of irradiance normalized earth radiances (albedos) for use in the ozone retrievals. Such

usage reduces system sensitivity to sensor throughput changes. In addition, the weekly solar irradiance measurements account for long-term solar variability.

The solar irradiances are also used in wavelength calibration and in the estimation of pixel-to-pixel gain variability. As noted above, these two processes are critical for proper on-orbit calibration of the OMPS instruments. Table 2 shows the derived solar calibration allocations which were flowed down from the top level requirements shown in Table 1. These allocations ensure that the data collected are of sufficient quality to provide the necessary corrections and calibrations. Integration times and frame co-adding are carefully chosen to provide the specified SNRs. Goniometric errors are related to ground measurement knowledge of the goniometric responses of each sensor as well as pointing knowledge on-orbit. Diffuser exposure requirements are specified to constrain on-orbit diffuser degradation due to solar exposure. The exposure requirements are derived from heritage diffuser degradation observed on previous missions using similar diffusers^{12,13}. The last requirement, calibration period, is driven by the period in orbit between the end of earth observations and the time that the spacecraft enters eclipse.

Table 2. Solar calibration derived allocations.

| Parameter | Required Value | Drives |
|-----------------------|------------------------------|--|
| Nadir | | |
| Solar SNR (per pixel) | > 1000 | Solar calibration operations |
| Goniometric errors | < 0.24% | Diffuser resolver accuracy, BRDF measurement |
| Diffuser exposure | < 180 seconds | Solar calibration operations |
| Calibration period | < 300 seconds | Solar calibration operations |
| Limb | | |
| Solar SNR (per pixel) | > 500 in UV > 1000 in Vis | Solar cal operations |
| Goniometric errors | < 0.24% | Diffuser resolver accuracy, BTDF measurement |
| Diffuser exposure | < 180 seconds/week | Solar calibration operations |
| Calibration period | < 148 seconds | Solar calibration operations |

The solar calibrations for each of the three instruments occur on different, though consecutive, orbits. On calibration orbits, the solar observations are taken immediately after earth observations are complete and before the spacecraft enters eclipse. Every six months, the reference diffuser is deployed for each instrument bracketed by two orbits during which working diffuser measurements are made. The reference and working diffuser solar observations are compared within the ground processing software to detect long-term working diffuser degradation as a function of time. This is primarily a monitoring process, but adjustments to the diffuser reflectivity or transmissivity terms are made in the calibration equations if necessary. During the initial early orbit checkout phase, more solar irradiance measurements are taken to establish the required baselines.

The nadir solar irradiance measurements are collected using a reflective ground aluminum diffuser similar to that used for TOMS and SBUV. The nadir sensor and a more detailed view of the calibration housing and mechanism are shown in Figure 1. The drawing on the right illustrates the nadir calibration mechanism. The entrance slit is near the top of the image with the diffuser deployed to the center position. Due to the wide 110 degree field-of-view of this instrument, the diffuser must be rotated through seven different overlapping positions to cover the full range of field angles. The diffuser itself covers roughly 20 degrees of the nadir field-of-view. At each position, the diffuser scatters sunlight into the nadir aperture. The ground processing applies the appropriate goniometric corrections and then pieces the seven data frames into one effective solar irradiance frame. When not in use, the diffusers are stowed to protect them from the space environment.

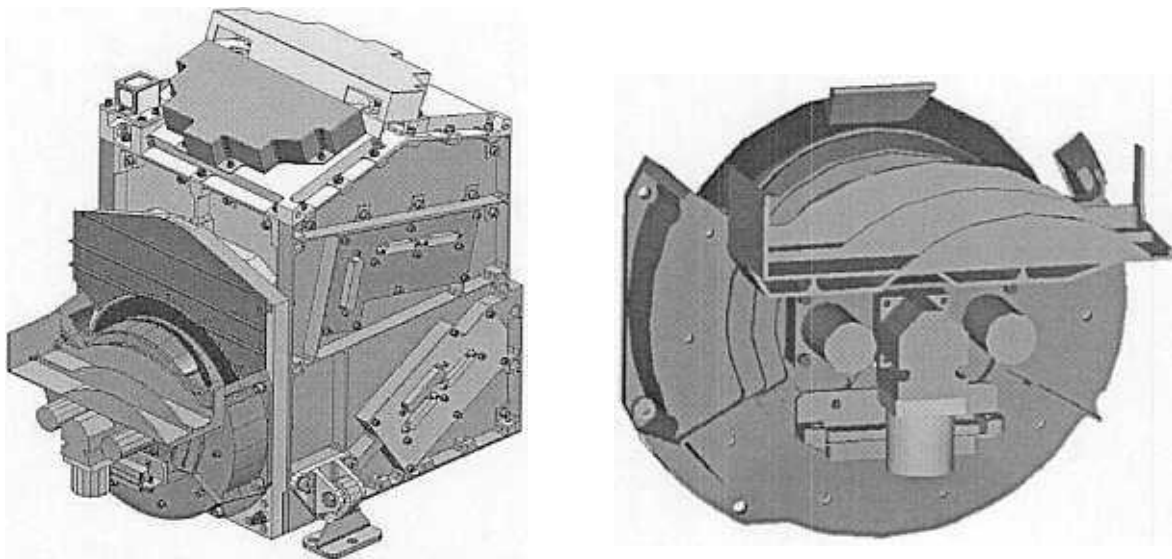


Figure 1. Diagram of the OMPS nadir sensor (left) and a detailed view of the nadir calibration housing and mechanism (right). As shown, the reflective diffuser is deployed in the center position.

Due to the different viewing geometry, the OMPS limb sensor utilizes transmissive diffusers to collect solar measurements. A similar approach was used on the Atmosphere Explorer 5 mission. The diffusers are constructed from two ground fused silica layers along with a microlens array to reduce the strong forward scattering of transmissive diffusers. This flattens the dependence of transmissivity on solar incidence angle. The diffusers are assembled in pairs with one diffuser covering the large aperture while the second diffuser covers the small aperture. The large aperture diffuser also includes a neutral density filter to equalize the solar signals observed from the large and small apertures. Figure 2 illustrates the OMPS limb profiler sensor as well as the calibration wheel with the housing removed. The image clearly shows the two diffuser pairs used for working and reference solar calibrations. Once per week, the working diffuser pair is rotated over each of the three entrance aperture pairs while the other apertures are blocked. On the ground, these data are corrected for goniometry, then assembled into one effective solar irradiance image for use in further SDR and EDR processing. Like the nadir instrument, the diffusers are stowed when not in use to minimize long-term degradation due to UV radiation and other space environment effects.

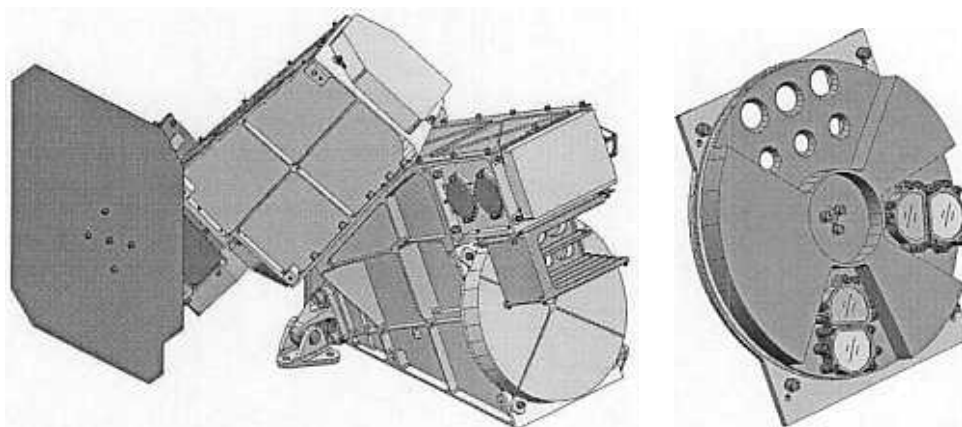


Figure 2. Diagram of the OMPS limb profiler sensor (left) and a detailed view of the limb calibration wheel with the housing removed (right). The working and reference transmissive diffusers are shown on the wheel along with the six entrance apertures.

2.3.2. Dark current measurements

As previously noted, the mean dark current signal must be removed to minimize impacts on top-level EDR performance. The CCDs are each operated at low temperatures to minimize the dark current in each focal plane. The nadir total column CCD is operated at -30 degrees C while the limb profile and nadir profile CCDs are operated -45 degrees C. The two profilers are operated at a lower temperature since these instruments are required to measure very weak radiances that are more susceptible to dark current noise. Thermo-electric coolers and radiators in each instrument design facilitate the temperature reductions. In addition, the temperatures are held within ± 0.1 degrees C to reduce thermal variations in dark current.

Dark current measurements are collected weekly immediately following the completion of solar irradiance observations. For each instrument, the integration time and number of frame co-adds are selected to ensure that the mean dark signal can be observed above the random dark noise and other noise sources. Over time, dark current is expected to rise due to long-term radiation damage to the detector. The design includes radiation shielding to minimize this effect, but weekly measurements are still required to track changes in the dark signal. As described in a previous section, the resultant dark current frames are used to correct the science data frames.

2.3.3. LED measurements

The ideal approach for linearity measurements is to have a known signal injected into each pixel. The readout then provides the output of the system and the resultant mapping from input to output can be determined as shown in Figure 3. However, in the absence of a perfectly calibrated source, one with stable output can be substituted. In this sense, precisely controlled integration time can be exchanged for absolute signal. With this in mind, the non-linearity of each OMPS instrument is measured using observations of direct LED illumination on each CCD. The LED approach provides relatively stable and uniform illumination of each focal plane. Two LEDs per focal plane are included in the OMPS design: one functions as the primary unit while the other is reserved as redundant backup in the event of a failure.

The LED measurement sequence is preceded by a five minute LED warm-up period to allow the LED output to stabilize. Lab tests indicate that this period is sufficient for the initial rapid decrease in LED flux to stabilize before linearity measurements are collected. Following the warm-up, LED measurements are collected at stepped integration times from zero to an integration time that results in detector saturation. The integration times are stepped in increments of 0.1 seconds and five frames are collected at each integration time. Sets of five reference frames are interleaved with the stepped frames to provide data for use in correcting for any residual LED drift during the measurement period. These data are transmitted to ground processing stations where the SDR algorithm computes the nonlinearity. Nonlinearity tables are then uploaded to the spacecraft for use in applying the nonlinearity correction to earth scene radiances in real time.

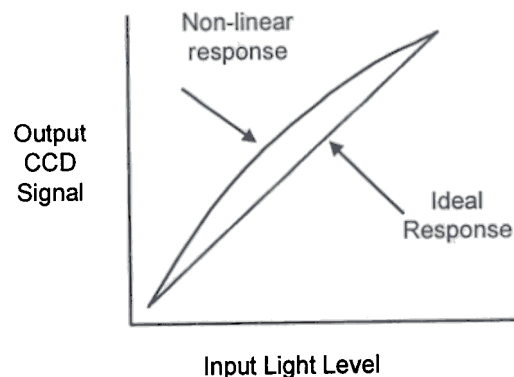


Figure 3. Hypothetical system nonlinearity compared to a perfectly linear response.

3. CONCLUSIONS

The OMPS sensors represent the next generation of operational sensors to monitor global total column and profile ozone. The sensor and algorithms build upon TOMS, SBUV, and SOLSE/LORE heritage to provide improved products that track the spatial and temporal dependence of global ozone. On-orbit calibration ensures the long-term accuracy and stability of these products. The OMPS design includes sensor design features that allow for the collection of on-orbit data required for radiometric and spectral calibration of the instruments. In addition, OMPS ground processing algorithms perform the required trending, monitoring, and calibration operations to reduce sensor effects in the radiances and irradiances provided to the EDR algorithms.

REFERENCES

1. C. S. Nelson and J. D. Cunningham, The National Polar-orbiting Operational Environmental Satellite System future U.S. environmental observing system, *Proceedings of the American Meteorological Society 82nd Annual Meeting*, paper 3.1, January 2002.
2. J. Hornstein, E.P. Shettle, R.M. Bevilacqua, S. Chang, E. Colon, L. Flynn, E. Hilsenrath, S. Mango, H. Bloom, and F. Sanner, The Ozone Mapping and Profiler Suite-Assimilation Experiment (OMPS-AE), IGARSS, II:809-812 2002.
3. M. Dittman, et al., Nadir ultraviolet imaging spectrometer for the NPOESS Ozone Mapping and Profiler Suite (OMPS), *Proc. SPIE*, 4814, 2002.
4. R.D. McPeters, P.K. Bhartia, A.J. Krueger, J.R. Herman, B.M. Schlesinger, C.G. Wellemeyer, C.J. Seftor, G. Jaross, S.L. Taylor, T. Swisler, O. Torres, G. Labow, W. Byerly, and R. P. Cebula, Nimbus-7 TOMS Ozone Mapping Spectrometer (TOMS) Data Products User's Guide, *NASA Reference Publication 1384*, April 1996.
5. A.J. Fleig, et al., Nimbus 7 Solar Backscatter Ultraviolet (SBUV) Ozone Products User's Guide, *NASA Reference Publication 1234*, 1990.
6. M.G. Dittman, et al, Limb Broad-Band Imaging Spectrometer for the NPOESS Ozone Mapping and Profiler Suite (OMPS), *Proc. SPIE*, Seattle, Washington, 2002.
7. R.D. McPeters, S. J. Janz, E. Hilsenrath, T. L. Brown, D. E. Flittner, and D. F. Heath, The retrieval of ozone profiles from limb scatter measurements: results from the Shuttle Ozone Limb Sounding Experiment, *Geophys. Res. Lett.*, 27, 2597-2600, 2000.
8. D.E. Flittner, B. M. Herman, and P. K. Bhartia, Ozone profiles retrieved from limb scatter measurements: theory, *Geophys. Res. Lett.*, 27, 2601-2604, 2000.
9. G. Jaross, et al., Calibration and postlaunch performance of the Meteor 3/TOMS instrument, *J. Geophys. Res.*, 100, 2985—2995, 1995.
10. C.J. Seftor., G. Jaross, J.R. Herman, X. Gu, L. Moy, S.L. Taylor, and C.G. Wellemeyer, The Meteor 3/total ozone mapping spectrometer version 7 data set: Calibration and analysis, *J. Geophys. Res.*, 102, 19247-19256, 1997.
11. R.D. McPeters, et al., Earth Probe Total Ozone Mapping Spectrometer (TOMS) Data Product User's Guide, *NASA/TP-1998-206895*, November 1998.
12. G. Jaross, A. J. Krueger, and C. G. Wellemeyer, Sensitivity of Total Ozone Mapping Spectrometer products to diffuse reflectance measurements, *Metrologia*, 35, 663-668, 1998.
13. G. Jaross, R. Cebula, M. DeLand, R. McPeters, E. Hilsenrath, and A. Krueger, Backscatter ultraviolet instrument solar diffuser degradation, *Proc. SPIE*, 3427, 432-444, 1998.
14. C. Caspar, and K. Chance, GOME Wavelength Calibration Using Solar and Atmospheric Spectra, *Proc. 3rd ERS Symposium (ESA SP-414)*, p. 609, 1997.